Inorg. Chem. **2008**, *47*, 7880−7887

Reactivity of Electrochemically Generated Rhenium (II) Tricarbonyl α-Diimine Complexes: A Reinvestigation of the Oxidation of Luminescent $Re(CO)_3$(α-Diimine)Cl and Related Compounds

John P. Bullock,*,†,‡ Eric Carter,‡ Ryan Johnson,† Abigail T. Kennedy,† Sarah E. Key,‡ Brian J. Kraft,‡ David Saxon,† and Patrick Underwood‡

The Division of Natural Science and Mathematics, Bennington College, Bennington, Vermont 05201, and The Department of Chemistry, Central Washington University, Ellensburg, Washington 98926

Received March 24, 2008

The oxidative electrochemistry of luminescent rhenium (I) complexes of the type $Re(CO)_3(LL)Cl$, **1**, and $Re(CO)_3(LL)Br$, **2**, where LL is an α-diimine, was re-examined in acetonitrile. These compounds undergo metal-based one-electron oxidations, the products of which undergo rapid chemical reaction. Cyclic voltammetry results imply that the electrogenerated rhenium (II) species $\mathbf{1}^+$ and $\mathbf{2}^+$ disproportionate, yielding $[Re(CO)_3(LL)(CH_3CN)]^+$, **7**, and additional products. Double potential step chronocoulometry experiments confirm that $\mathbf{1}^+$ and $\mathbf{2}^+$ react via second-order processes and, furthermore, indicate that the rate of disproportionation is influenced by the basicity and steric requirements of the α-diimine ligands. The simultaneous generation of rhenium (I) and (III) carbonyl products was detected upon the bulk oxidation of **1** using infrared spectroelectrochemistry. The rhenium (III) products are assigned as $[Re(CO)_3(LL)Cl_2]^+$, **5**; an inner-sphere electron-transfer mechanism of the disproportionation is proposed on the basis of the apparent chloride transfer. Chemically irreversible two-electron reduction of **5** yields **1** and Cl^-. No direct spectroscopic evidence was obtained for the generation of rhenium (III) tricarbonyl bromide disproportionation products, $[Re(CO)_3(LL)Br_2]^+$, **6**; this is attributed to their relatively rapid decomposition to **7** and dibromine. In addition, the 17-electron radical cations, $\mathbf{7}^+$, were successfully characterized using infrared spectroelectrochemistry.

Introduction

Rhenium tricarbonyl complexes of α-diimine ligands (LL) have been extensively studied since their luminescent properties were initially characterized more than 30 years ago.[1] Many of these complexes show strong room-temperature emissions that result from decay of metal-to-ligand charge transfer (MLCT) excited states.[2] Their excited-state lifetimes, photochemical stability, and robust nature make them promising candidates for a wide range of applications such as building blocks in supramolecular assemblies,[3] various sensing technologies,[3c,4] luminescent probes for long-range electron-transfer studies in proteins and other biomolecular systems,[5] and light-emitting electronic devices.[6] Interest in these compounds remains strong as evidenced by a number of recent reviews.[7] Elucidation of the redox characteristics of these and related compounds can yield insight into their photophysical and photochemical properties,[8] and, accordingly, their electrochemical oxidations and reductions have been widely investigated. These studies indicate that most compounds of the type $[Re(CO)_3(LL)X]^+$ (**1** and **2**, see Table

* To whom correspondence should be addressed. E-mail: jbullock@bennington.edu.

† Bennington College.

‡ Central Washington University.

(1) Wrighton, M.; Morse, D. L. *J. Am. Chem. Soc.* **1974**, *96*, 998–1003.

(2) Caspar, J. V.; Meyer, T. J. *J. Phys. Chem.* **1983**, *87*, 952–957.

(3) (a) Balzani, V.; Juris, A.; Ventyri, M.; Campagna, S.; Serroni, S. *Chem. Rev.* **1996**, *96*, 759–833. (b) Ashton, P. R.; Balzani, V.; Kocian, O.; Prodi, L.; Spencer, N.; Stoddart, J. F. *J. Am. Chem. Soc.* **1998**, *120*, 11190–11191. (c) Sun, S.-S.; Lees, A. J. *Coord. Chem. Rev.* **2002**, *230*, 170–191. (d) Kleineweischede, A.; Mattay, J. *J. Organomet. Chem.* **2006**, *691*, 1834–1844.

(4) (a) Shen, Y.; Sullivan, B. P. *Inorg. Chem.* **1995**, *34*, 6235–6236. (b) Higgins, B.; DeGraff, B. A.; Demas, J. N. *Inorg. Chem.* **2005**, *44*, 6662–6669. (c) Cattaneo, M.; Fagalde, F.; Katz, N. E. *Inorg. Chem.* **2006**, *45*, 6884–6891.

(5) (a) Connick, W. B.; Di Bilio, A.; Hill, M. G.; Winkler, J. R.; Gray, H. B. *Inorg. Chim. Acta* **1995**, *240*, 169–173. (b) Lo, K. K.-W.; Tsang, K. H.-K.; Hui, W. K.; Zhu, N. *Chem. Commun.* **2003**, 2704–2705. (c) Dunn, A. R.; Belliston-Bittner, W.; Winkler, J. R.; Getzoff, E. D.; Stuehr, D. J.; Gray, H. B. *J. Am. Chem. Soc.* **2005**, *127*, 5169–5179.

(6) (a) Wang, K.; Huang, L.; Gao, L.; Jin, L.; Huang, C. *Inorg. Chem.* **2002**, *41*, 3353–3358. (b) Si, Z.; Li, J.; Li, B.; Zhao, F.; Liu, S.; Li, W. *Inorg. Chem.* **2007**, *46*, 6155–6163.

10.1021/ic800530n CCC: $40.75
Published on Web 08/06/2008

Table 1. Numbering Scheme Employed for Starting Compounds and Electrogenerated Species

General Structural Formula	Number Designation	
	X = Cl^-	X = Br^-
$[Re(CO)_3(LL)X]^+$	**1**	**2**
$\{[Re(CO)_3(LL)](\mu\text{-}X)[Re(CO)_3(LL)X]\}^{2+}$	**3**	**4**
$[Re(CO)_3(LL)X_2]^+$	**5**	**6**
$[Re(CO)_3(LL)(CH_3CN)]^+$	**7**	

α-diimine letter designations: 2,2′-bipyridine (bpy), **a**; 4,4′-dimethyl-2,2′-bipyridine (dmb), **b**; 1,10-phenanthroline (phen), **c**; 4,7-dimethyl-1,10-phenanthroline (dmp), **d**; 5-chloro-1,10-phenanthroline (Cl-phen), **e**; 5-nitro-1,10-phenanthroline (NO_2-phen), **f**; 2,9-dimethyl-1,10-phenanthroline (or neocuproine, ncp), **g**. When no letter designation is used in the text, the behavior of all complexes of a given type can be assumed to show similar behavior.

1 for the numbering scheme employed in this work), undergo irreversible metal-based one-electron oxidations, and one-electron reductions that are centered on the α-diimine,[9] many of which have been shown to be chemically reversible. Indeed, some of the one-electron reduction products have been spectroscopically characterized using UV−vis, infrared, and ESR spectroelectrochemical techniques.[10,11] The cathodic processes are also of interest as certain complexes of this type have been shown to electrocatalytically reduce carbon dioxide.[12]

Products of the anodic processes, on the other hand, can potentially mimic the formally oxidized metal center formed upon generation of the MLCT state;[8d] species with such electron holes have been shown to be powerful oxidants,[13] and, by accepting electrons from sacrificial donors such as triethanolamine, play an important role in the photocatalytic reduction of carbon dioxide.[14] The chemical irreversibility of these processes indicates that the electrogenerated species react rapidly on the cyclic voltammetry time scale. As applications involving photooxidation steps require the reaction of photogenerated rhenium (II) centers with desired substrates to proceed at substantially greater rates than those of competing pathways, examination of the chemical reactions coupled to the anodic processes of these compounds can provide insight concerning the trends in reactivity for photogenerated rhenium (II) tricarbonyl species. In the course of examining the oxidation of these compounds, however, we found that relevant literature discussions concerning the reactions of the 17-electron electrogenerated species were inconsistent with a number of key observations. We therefore undertook a series of studies to better characterize this chemistry.

This report summarizes our work on this important class of luminescent compounds in acetonitrile. We have elucidated the reaction pathways undertaken by the rhenium (II) electrogenerated species ($\mathbf{1}^+$ and $\mathbf{2}^+$) and thereby provide a new interpretation of the frequently reported cyclic voltammetric responses of these compounds. In addition we propose a mechanistic scheme for several aspects of these reactions and discuss relevant supporting evidence collected in our laboratory. Finally, we present infrared characterization data of the rhenium (II) tricarbonyl radical cations, $[Re(CO)_3(LL)(CH_3CN)]^{2+}$, $\mathbf{7}^+$, to our knowledge the first such spectral characterization of the one-electron oxidation products of luminescent rhenium tricarbonyl compounds.

Experimental Section

Materials. Rhenium starting materials, $Re(CO)_5Cl$ and $Re(CO)_5Br$ (Strem) and ligands bpy, dmb (Alfa-Aesar), phen, ncp (Aldrich), dmp, Cl-phen, and NO_2-phen (GFS) were used as received. Halide complexes, **1a**−**g** and **2a**−**g**, and triflate salts of acetonitrile adducts, **7a**−**e**,**g**, were prepared and purified according to literature methods.[15] Electrochemical experiments were performed in acetonitrile (Pharmco, HPLC grade) using 0.1 M tetrabutylammonium hexafluorophosphate, TBAH (Sigma), as the supporting electrolyte. Electrolyte solutions were dried over activated 4 Å molecular sieves prior to use.

Equipment. Electrochemical experiments were performed with a Bioanalytical Systems CV-50 W Voltammetric Analyzer at room temperature using a glassy carbon working electrode (area = 0.071 cm^2) and a Ag/AgCl reference ($E_{1/2}$ value of the ferrocene/ferrocenium couple in acetonitrile was 420 mV with a peak separation of 88 mV at 100 mV/s). Solutions were purged with nitrogen presaturated with dried solvent. Double potential step chronocoulometry experiments were performed for bulk oxidation processes at step times, τ, ranging from 50 to 5000 ms using 0.5 to 2.5 mM solutions of **1** or **2**. Experiments employed a 400 mV potential step that was centered about the estimated $E_{1/2}$ values for each complex examined. Observed rate constants, k_{obs} were estimated by fitting Q_r/Q_f versus log $k_{obs}[Re]\tau$ plots to the theoretical working curve[16] of a second order radical coupling mechanism. Infrared spectroelectrochemical experiments were performed at room temperature using a cell equipped with a gold-mesh working electrode, a platinum-wire auxiliary electrode, a silver-wire pseu-

(7) (a) Vlček, A., Jr.; Busby, M. *Coord. Chem. Rev.* **2006**, *250*, 1755–1762. (b) Lo, K. K.-W.; Hui, W.-K.; Chung, C.-K.; Tsang, K. H.-K.; Lee, T. K.-M.; Li, C.-K.; Lau, J. S.-Y.; Ng, D. C.-M. *Coord. Chem. Rev.* **2006**, *250*, 1724–1736. (c) Kirgan, R. A.; Sullivan, B. P.; Rillema, D. P. *Top. Curr. Chem.* **2007**, *281*, 45–100.

(8) (a) Juris, A.; Campagna, S.; Bidd, I.; Lehn, J.-M.; Ziessel, R. *Inorg. Chem.* **1988**, *27*, 4007–4011. (b) Ciana, L. D.; Dressick, W. J.; Sandrini, D.; Maestri, M.; Ciano, M. *Inorg. Chem.* **1990**, *29*, 2792–2798. (c) Wallace, L.; Rillema, D. P. *Inorg. Chem.* **1993**, *32*, 3836–3843. (d) Vlček, A., Jr. *Chemtracts − Inorg. Chem.* **1993**, *5*, 1–35. (e) Stoyanov, S. R.; Villegas, J. M.; Rillema, D. P. *Inorg. Chem.* **2002**, *41*, 2941–2945.

(9) Luong, J. C.; Nadjo, L.; Wrighton, M. S. *J. Am. Chem. Soc.* **1978**, *100*, 5790–5795.

(10) Christensen, P; Hamnett, A.; Muir, A. V.; Timney, J. A. *J. Chem. Soc., Dalton Trans.* **1992**, 1455–1463.

(11) (a) Stor, G. J.; Hartl, F.; van Outersterp, J. W. M.; Stufkens, D. J. *Organometallics* **1995**, *14*, 1115–1131. (b) Lee, Y. F.; Kirchhoff, J. R.; Berger, R. M.; Gosztola, D. *J. Chem. Soc., Dalton Trans.* **1995**, 3677–3682. (c) Berger, S.; Klein, A.; Kaim, W.; Fiedler, J. *Inorg. Chem.* **1998**, *37*, 5664–5671. (d) Howell, S. L.; Scott, S. M.; Flood, A. H.; Gordon, K. C. *J. Phys. Chem. A* **2005**, *109*, 3745–3753.

(12) (a) Sullivan, B. P.; Bolinger, C. M.; Conrad, D.; Vining, W. J.; Meyer, T. J. *J. Chem. Soc., Chem. Commun.* **1985**, 1414–1416. (b) Johnson, F. P. A.; George, M. W.; Hartl, F.; Turner, J. J. *Organometallics* **1996**, *15*, 3374–3387.

(13) Reece, S. Y.; Nocera, D. G. *J. Am. Chem. Soc.* **2005**, *127*, 9448–9458.

(14) (a) Hawecker, J.; Lehn, J.-M.; Ziessel, R. J. *J. Chem. Soc., Chem. Commun.* **1983**, 536–538. (b) Kutal, C.; Weber, M. A.; Ferraudi, G.; Geiger, D. *Organometallics* **1985**, *4*, 2161–2166. (c) Sung-Suh, H. M.; Kim, D. S.; Lee, C. W.; Park, S.-E. *Appl. Organomet. Chem.* **2000**, *14*, 826–830. (d) Hori, H.; Takano, Y.; Koike, K.; Sasaki, Y. *Inorg. Chem. Commun.* **2003**, 300. (e) Kurz, P.; Probst, B.; Spingler, B.; Alberto, R. *Eur. J. Inorg. Chem.* **2006**, 2966.

(15) Sacksteder, L.; Zipp, A. P.; Brown, E. A.; Sterich, J.; Demas, J. N.; DeGraff, B. A. *Inorg. Chem.* **1990**, *29*, 4335–4340.

(16) Hanafey, M. K.; Scott, R. L.; Ridgeway, T. H.; Reilley, C. N. *Anal. Chem.* **1978**, *50*, 116–137.

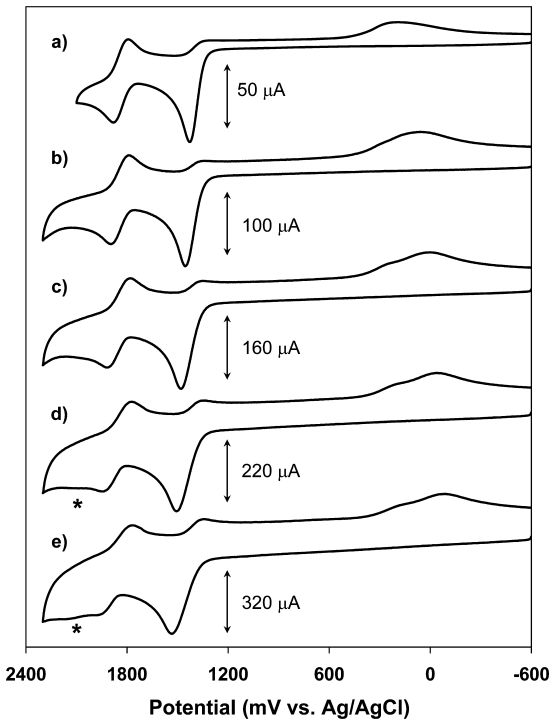

Figure 1. Cyclic voltammograms of 1.9 mM **1d** in CH_3CN/TBAH at (a) 250 mV/s, (b) 1,000 mV/s, (c) 2,500 mV/s, (d) 5,000 mV/s, and (e) 10,000 mV/s. The broad peak observed at high scan rates (marked with the asterisk in traces 1d and 1e) is assigned to the dinuclear chloride-bridged intermediate, **3d**, in Scheme 1.

doreference, and CaF_2 windows;[17] potentials employed for thin-layer bulk oxidation processes were typically 200−300 mV more positive than the peak potentials observed by cyclic voltammetry. Infrared spectra were collected using a Nicollet Avatar 370 FTIR.

Results & Discussion

Oxidation of $Re(CO)_3(LL)Cl$. The cyclic voltammogram of **1d** in CH_3CN/TBAH obtained at a scan rate of 250 mV/s is shown in part a of Figure 1. The main features include an irreversible anodic peak at 1380 mV vs Ag/AgCl, assigned to the one-electron oxidation of the bulk species to $\mathbf{1d}^+$ and two coupled peaks: a reversible, but smaller, oxidation ($E_{1/2}$ = 1790 mV), and a broad reduction with a peak maximum at 220 mV. Similar behavior has been reported by numerous laboratories for this class of compounds as well as for the analogous bromide and cyanide derivatives.[3d,6b,8a,9,10,18] Oxidation potentials for the bulk and coupled peaks of complexes examined in this study are presented in Table 2. These are in good agreement with previous reports and correlate well with the electron donating or withdrawing abilities of the α-diimine substituents as described elsewhere.[8c,18g]

It is generally accepted that the anodic peak coupled to the bulk oxidation, which was characteristic of all complexes of type **1** examined in this study, is due to the reversible one-electron oxidation of $[Re(CO)_3(LL)(CH_3CN)]^+$, **7**, the generation of which has been confirmed spectroscopically.[10] The mechanism commonly cited[10,18b,g,h,19] to explain its production involves a unimolecular process in which the chloride ligand serves as a one-electron reductant toward the electrogenerated rhenium (II) center, resulting in the loss of chlorine radical from the complex (which then forms molecular chlorine) and subsequent coordination by the solvent (eq 1). However, no detection of either chlorine radical or molecular chlorine has been reported in these systems. Nor does this reaction pathway account for the fact that the coupled oxidation peak consistently has a lower current than the bulk peak. For example, in part a of Figure 1, the current ratio of the coupled to the bulk anodic peaks (hereafter referred to as $i_{a,c}/i_{a,b}$) is 0.44. The fact that this ratio is considerably less than 1 cannot be due to slow kinetics of the coupled reaction, as a slow process would not result in such marked irreversibility of the bulk oxidations. Indeed, as Wrighton and co-workers reported for **1c**, scan rates upward of 50 000 mV/s are necessary to achieve chemical reversibility of the bulk oxidation.[9]

$$1^+ + CH_3CN \rightarrow 7 + \tfrac{1}{2}\,Cl_2 \qquad (1)$$

To better characterize the current relationships between the two anodic peaks, we examined the peak current ratios obtained in a series of scan rate studies of **1** in acetonitrile. Parts a−e of Figures 1, which show selected cyclic voltammograms for the scan rate study of **1d**, indicate a clear dependence of $i_{a,c}/i_{a,b}$ on scan rate; the ratio decreases from 0.44 at 250 mV/s to 0.32 at 10 000 mV/s. When the scan rate was decreased further (not shown), $i_{a,c}/i_{a,b}$ increased to 0.46 at 100 mV/s and 0.49 at 25 mV/s. Thus, at sufficiently low scan rates, the current of the coupled oxidation peak appears to approach ∼50% that of the bulk process, indicating that only half of the initially generated Re^{2+} species is ultimately converted to **7**. It is therefore highly likely that $\mathbf{1}^+$ disproportionates rather than undergoes a unimolecular reduction by the chloride ligand as implied by eq 1. These data are representative of all compounds of type **1** examined in this work except the sterically hindered ncp complex, **1g**. This chemistry is consistent with the known propensity toward disproportionation of other d^5 carbonyl complexes.[20]

Because the rhenium (I) disproportionation products are not the initial chlorides, **1**, but instead the corresponding

(17) The infrared spectroelectrochemical cell employed in this work is a slightly modified version of that described in Bullock, J. P.; Boyd, D. C.; Mann, K. R *Inorg. Chem.* **1987**, *26*, 3084–3086.

(18) (a) Breikss, A. L.; Abruña, H. D. *J. Electroanal. Chem.* **1986**, *201*, 347–358. (b) O'Toole, T. R.; Sullivan, B. P.; Bruce, M. R.-M.; Margerum, L. D.; Murray, R. W.; Meyer, T. J. *J. Electroanal. Chem.* **1989**, *259*, 217–239. (c) Sahai, R.; Rillema, D. P.; Shaver, R.; Van Wallendael, S.; Jackman, D. C. *Inorg. Chem.* **1989**, *28*, 1022–1028. (d) Van Wallendael, S.; Shaver, R.; Rillema, D. P.; Yoblinski, B. J.; Stathis, M.; Guarr, T. F. *Inorg. Chem.* **1990**, *29*, 1761–1767. (e) Moya, S. A.; Pastene, R.; Schmidt, R.; Guerrero, J.; Sartori, R. *Polyhedron* **1992**, *11*, 1665–1670. (f) Moya, S. A.; Guerrero, J.; Pastene, R.; Schmidt, R.; Sariego, R.; Sartori, R.; Aparicio, J. S.-A.; Fonseca, I.; Martinez-Ripoll, M. *Inorg. Chem.* **1994**, *33*, 2341–2346. (g) Richter, M. M.; Debad, J. D.; Striplin, D. R.; Crosby, G. A.; Bard, A. J. *Anal. Chem.* **1996**, *68*, 4370–4376. (h) Paolucci, F.; Marcaccio, M.; Paradisi, C.; Roffia, S.; Bignozzi, C. A.; Amatore, C. *J. Phys. Chem. B* **1998**, *102*, 4759–4769. (i) Kirgan, R.; Simpson, M.; Moore, C.; Day, J.; Bui, L.; Tanner, C.; Rillema, D. P. *Inorg. Chem.* **2007**, *46*, 6464–6472.

(19) Hino, J. K.; Della Ciana, L.; Dressick, W. J.; Sullivan, B. P. *Inorg. Chem.* **1992**, *31*, 1072–1080.

(20) Bond, A. M.; Colton, R. *Coord. Chem. Rev.* **1997**, *166*, 161–180.

Table 2. Summary of Electrochemical and Kinetic Data of $Re(CO)_3(LL)X$ Complexes in CH_3CN/TBAH[a]

LL	complex number	$E_{p,a,bulk}$	$E_{1/2,\ coupled}$[b]	$i_{a,c}/i_{a,b}$[c]	$E_{p,\ c,\ coupled}$[d]	k_{obs} ($M^{-1}s^{-1}$)[e]
X = Cl						
bpy	**1a**	1410	1820	0.44	220, *10*	40 000
dmb	**1b**	1380	1800	0.42	250, *10*	55 000
phen	**1c**	1410	1840	0.46	340, *70*	50 000
dmp	**1d**	1380	1790	0.46	220, *0*	90 000
Cl−phen	**1e**	1420	1840	0.48	390, *140*	45 000
NO_2−phen	**1f**	1460	1870	0.44	470, *270*	24 000
ncp	**1g**	1460	1870	0.45	570	1200
X = Br[f]						
bpy	**2a**	1400	1820	0.49	680	70 000
dmb	**2b**	1380	1800	0.50	730	90 000
NO_2−phen	**2f**	1440	1860	0.56	720	24 000

[a] Potentials are expresses as mV vs Ag/AgCl; all scan rates are 100 mV/s unless otherwise noted. [b] $E_{1/2}$ values correspond to the corresponding disproportionation product, **7**, generated after oxidation of the bulk species. [c] Peak current ratio of the coupled oxidation of **7** to the bulk process at 100 mV/s. [d] Potentials of coupled reduction peaks; those of transient species (in italics) were measured at scan rates of 2500 mV/s. [e] Observed rate constants for the disproportionation of $\mathbf{1}^+$ and $\mathbf{2}^+$ as determined by double potential step chronocoulometry; estimated uncertainty is ±15%. [f] Examination of bromide complexes **2c**−**e**, **g** was precluded due to poor solubility in CH_3CN.

Scheme 1. Proposed Disproportionation Mechanism for Electrogenerated $\mathbf{1}^+$ and $\mathbf{2}^{+a}$

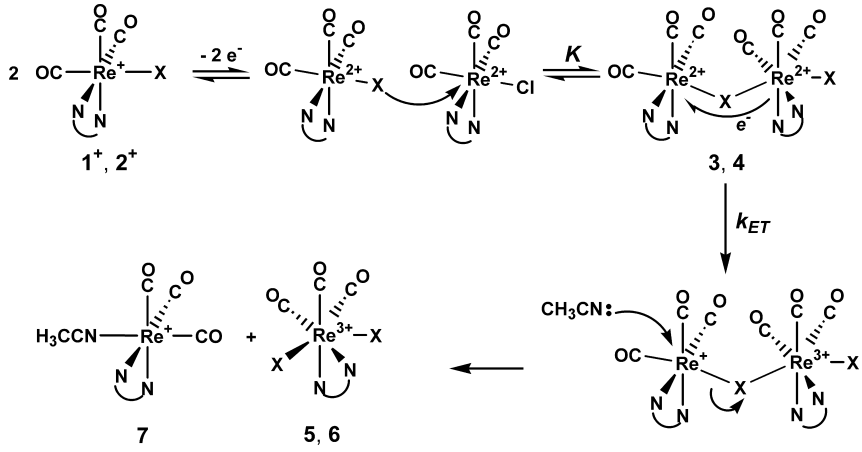

[a] X = Cl^- in structures $\mathbf{1}^+$, **3** and **5**, and Br^- in $\mathbf{2}^+$, **4**, and **6**. The experimentally measured rate constant, k_{obs}, is equal to Kk_{ET} in this scheme.

acetonitrile adducts, **7**, the likely mechanism involves a chloride-transfer step. Accordingly, we propose that the disproportionation takes place via the inner-sphere mechanism outlined in Scheme 1. In this reaction sequence, the electron-transfer step is preceded by a rapid equilibrium involving the formation of a chloride-bridged dinuclear intermediate, **3**. This species consists of formal 19-electron, 7-coordinate,[21] and 17-electron, 6-coordinate rhenium centers. Electron transfer via the chloride bridge then yields two 18-electron moieties. The chloride transfer takes place as the chloride-rhenium (I) bond is cleaved in an associative ligand substitution pathway involving the solvent.[22] This reaction sequence would then result in **7** and the 7-coordinate rhenium (III) complex, $[Re(CO)_3(LL)Cl_2]^+$, **5**.

We have collected the following experimental evidence in support of the mechanism outlined in Scheme 1: chronocoulometric data confirm that decomposition of electrogenerated $\mathbf{1}^+$ takes place via a second order process, cyclic voltammetric experiments reveal a short-lived intermediate that is formed *prior* to formation of the acetonitrile adduct, and infrared spectroelectrochemical data show that corresponding **5** and **7** are simultaneously generated upon oxidation of **1**. The chronocoulometric data is discussed later in this article, but the other two pieces of supporting evidence are presented here. Cyclic voltammetry experiments of **1d** performed at high scan rates reveal a broad but definable peak (at 2200 mV in part e of Figure 1) approximately 200 mV positive of the peak due to **7d**. We assign this to the oxidation of the intermediate of the inner-sphere electron transfer mechanism, **3d**.[23] Of particular importance is the fact that the current due to oxidation of **7d** decreases relative to that due to **3d** as the scan rate increases, indicating that **7d** is formed after **3d**.

We observed peaks attributable to chloride-bridged intermediates, **3**, for all complexes of type **1** examined in this study. The sterically congested **3g**, however, is considerably longer-lived than any of the others, being distinctly observable at scan rates as low as 100 mV/s. We interpret the

(21) Seven-coordinate, 19-electron species have ample precedent and are commonly postulated intermediates in associative substitution pathways involving electrogenerated 17-electron species. See (a) Tyler, D. R. *Prog. Inorg. Chem.* **1988**, *36*, 125–194. (b) Zhang, Y.; Gosser, P. H.; Rieger, P. H.; Sweigert, D. A. *J. Am. Chem. Soc.* **1991**, *113*, 4062–4068. (c) Delville-Desbois, M.-H.; Varret, F.; Astruc, D. *J. Chem. Soc., Chem. Commun.* **1995**, 249–250.

(22) Haim, A. *Acc. Chem. Res.* **1975**, *8*, 264–272.

(23) We speculate that the oxidation is centered on the 18-electron rhenium(I) moiety produced by the electron transfer; the peak potential is roughly 700 mV positive of the bulk process, consistent with the expected decrease in basicity of the chloride that results from its role as a bridging ligand.

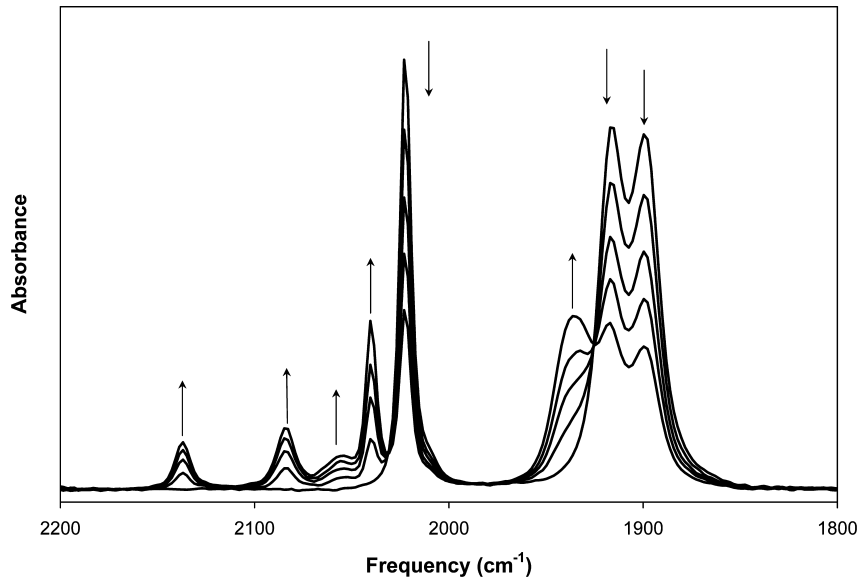

Figure 2. Infrared spectral changes in the carbonyl stretching region observed upon oxidation of **1a** in CH_3CN/TBAH; the total elapsed time of the sequence was 2 min. Products are assigned as **5a** and **7a**.

Table 3. Carbonyl Stretching Frequencies of $Re(CO)_3(LL)Cl$ Complexes and Related Species[a]

	Structure Type			
LL	**1**	**5**	**7**	$\mathbf{7}^+$
a (bpy)	2022, 1916, 1899	2137, 2084, 2056	2040, 1937	2124, 2061, 2026
b (dmb)	2021, 1914, 1896	2136, 2082, 2055	2039, 1934	2122, 2059, 2016
c (phen)	2023, 1917, 1900	2136, 2084, 2058	2040, 1938	2124, 2060, 2017
d (dmp)	2021, 1914, 1896	2135, 2082, 2055	2039, 1934	2120, 2059, 2017
e (Cl−phen)	2024, 1919, 1902	2138, 2086, 2057	2042, 1939	2125, 2065, 2031
f (NO_2−phen)	2025, 1920, 1904	2139, 2088, 2060	2043, 1941	[b]
g (ncp)	2022, 1910 (sh), 1900	2121, 2079, 2052	2039, 1938, 1930 (sh)	2121, 2059, 2015

[a] All data were collected in CH_3CN/TBAH. Spectra of complexes of type **7** were obtained from solutions of the triflate salts, except for the **7f**, which was generated electrochemically from **1f**. Complexes of type **5** and $\mathbf{7}^+$ were generated electrochemically. [b] Not measured.

enhanced kinetic stability of **3g** as support for the suggestion that the decomposition pathway followed by **3** is associative in nature, as such a pathway would be less facile for **3g** given the steric congestion resulting from the methyl substituents at the two and nine positions of the phenanthroline ligand.[24]

Spectroscopic evidence in support of the reactions outlined in Scheme 1 comes from infrared spectroelectrochemical experiments. Figure 2 shows the spectral changes in the carbonyl stretching region that are observed upon thin-layer bulk electrolysis of **1a**. Five peaks are seen to grow isosbestically during the electrolysis. Two of these (at 2040 and 1937 cm^{-1}) are assigned to **7a**,[25] whereas the pattern and relative intensities of the three other peaks are similar to those of 7-coordinate d^4 tricarbonyl complexes such as $[Mo(CO)_3(LL)(CH_3CN)_2]^{2+}$,[26] and $M(CO)_3(PP)X_2$,[27] where M is either Mo^{2+} or W^{2+}, PP is a chelating group 15 donor ligand such a diphosphine, and X is Cl^-, Br^-, or I^-. On this basis, and on the observed increase in the carbonyl stretching frequencies, we assign these three peaks to the rhenium (III) disproportionation product, $[Re(CO)_3(bpy)Cl_2]^+$, **5a**. Spectral data similar to those shown in Figure 2 were collected all other complexes of type **1** and are summarized in Table 3.

Disproportionation Rate Studies. Using double potential step chronocoulometry[28] we measured the observed disproportionation rate constants, k_{obs} (equal to Kk_{ET} in Scheme 1), of several complexes of types **1** and **2** to ascertain the effects that various structural features have on the reaction kinetics; results are presented in Table 2. Factors studied included the steric demands and basicity of the α-diimine ligands and the identity of the halide. The measured charge ratios, Q_r/Q_f, were found to depend on both the step time and the rhenium concentration, indicating that the chemical reaction coupled to the electrode process is second order with respect to electrogenerated Re^{2+}.[16] An example, showing the data obtained for **1f**, is shown in Figure 3. The rate constant estimated from these data is 24 000 $M^{-1}s^{-1}$ with an uncertainty of approximately ± 15%.

The disproportionation rate constants in Table 2 reveal several trends. First, there is a correlation between k_{obs} and

(24) (a) Smith, G. F.; McCurdy, W. H., Jr. *Anal. Chem.* **1952**, *24*, 371–373. (b) Pallenberg, A. J.; Koenig, K. S.; Barnhart, D. M. *Inorg. Chem.* **1995**, *34*, 2833–2840.

(25) The relative intensities of product peaks assigned to **7a** are consistent with a disproportionation; the data in Figure 2 indicate that 0.48 mol of **7a** are generated per mol of **1a** consumed. Data similar to those shown in Figure 2 have been reported previously.[10] In that work, oxidation of **1b** in acetonitrile was shown to generate **7b** and another species the authors assigned as $[(\eta^6\text{-dmb})Re(CO)_3]^+$, a complex in which one of the two dmb rings bonds to the rhenium center as an arene ligand.

(26) Johnson, R.; Madhani, H.; Bullock, J. P. *Inorg. Chim. Acta* **2007**, *360*, 3414–3423.

(27) Bond, A. M.; Colton, R.; Jackowski, J. J. *Inorg. Chem.* **1978**, *17*, 105–111.

(28) Therien, M. J.; Ni, C.-L.; Anson, F. C.; Osteryoung, J. G.; Trogler, W. C. *J. Am. Chem. Soc.* **1986**, *108*, 4037–4042.

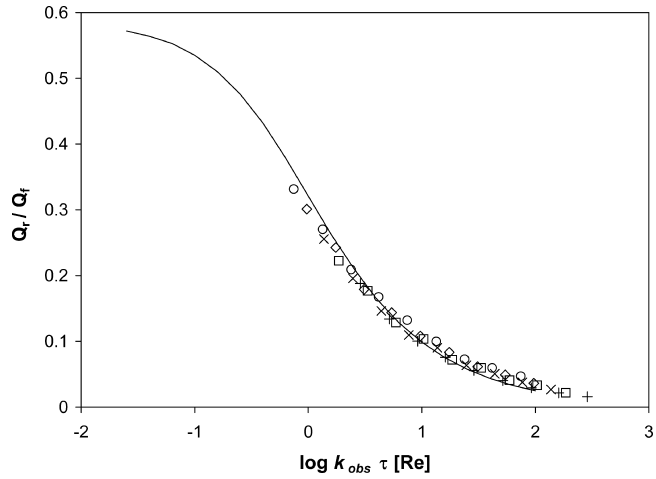

Figure 3. Double potential step chronocoulometry data obtained using 0.62 (○), 0.81 (◇), 1.14 (×), 1.54 (□), and 2.40 mM (+) **1f** at step times, τ, ranging from 50 msec to 5000 msec; initial and final potentials were 1190 and 1590 mV, respectively. The solid line represents the theoretical working curve from reference 16.

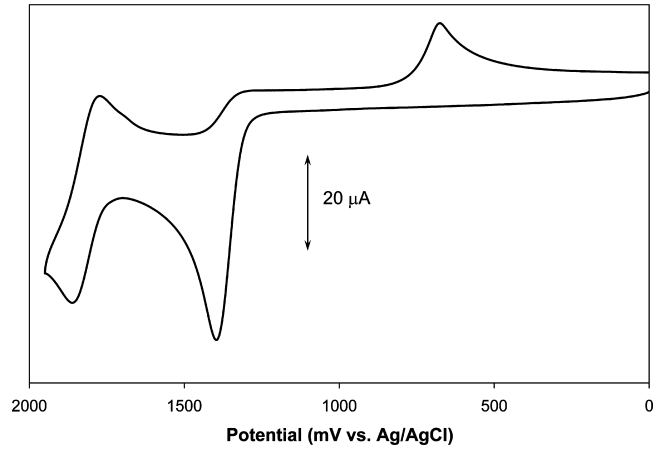

Figure 4. Cyclic voltammogram of 1.9 mM **2a** in CH_3CN/TBAH obtained at a scan rate of 100 mV/s. The coupled oxidation process is assigned to **7a**, whereas the coupled reduction is assigned to the two-electron reduction of $[Re(CO)_3(bpy)(\eta^1\text{-}Br_2)]^+$.

the electron donating or withdrawing properties of the substituents of the diimine ligands, with complexes of those bearing electron-donating groups reacting more rapidly. For example, the dmp complex, $\mathbf{1d}^+$, has a rate constant that is roughly four times that of the NO_2−phen complex, $\mathbf{1f}^+$. This is likely due to stabilization of the electron-deficient chloride-bridged intermediate, **3**, by electron-releasing substituents on the α-diimine ligand.[29] A second, much larger, effect on k_{obs} arises from steric demands of the diimine ligand. Specifically, k_{obs} for the disproportionation of $\mathbf{1g}^+$, is 1200 $M^{-1}s^{-1}$, a factor of 75 lower than that measured for the isomeric dmp complex, $\mathbf{1d}^+$. The smaller reaction rate is reflected by appreciably greater reversibility of the bulk oxidation peak in cyclic voltammetry experiments, an observation that had been reported previously without comment.[18g] We attribute the lower reaction rate to the same steric crowding of the metal center by the ncp ligand that inhibits attack by acetonitrile on the intermediate, **3g**, as discussed earlier.

We did not detect a clear effect of the bridging ligand on k_{obs}.[30] These studies were limited in scope, however, due to the poor solubility of bromide derivatives **2c**−**e** and **2g**.

Reduction of Rhenium (III) Chloride Disproportionation Products. Cyclic voltammetry data indicate that formation of **5** is more complex than the isosbestic spectral changes in Figure 2 imply. Specifically, scan rate studies (Figure 1) show two reduction processes coupled to the bulk oxidation. At 2500 mV/s, for example, **1d** shows a broad coupled reduction peak centered at about 10 mV with a distinct shoulder at 220 mV. Interestingly, the current ratio of these processes does not change appreciably as the scan rate increases. At lower scan rates, however, the current of the peak at lower potential is seen to decrease relative to that of the shoulder. At 250 mV/s, the peak at 10 mV is no longer clearly discernible but it does contribute to the elongated shape of the coupled reduction peak at 220 mV. We speculate that the two cathodic peaks observed at higher scan rates are due to isomeric forms of **5d** that are simultaneously generated by the disproportionation. A process akin to the *fac*-/*mer*- isomerizations that occur on the cyclic voltammetry time-scale in related species[31] could convert one form into the other and thereby be responsible for the observed changes in relative peak currents observed at lower scan rates.

We assign the coupled cathodic peaks to the irreversible two-electron reduction of **5d**, yielding **1d** and free chloride (eq 2). In support of this assignment, we have evidence that free chloride is generated upon reduction of **5d**. Specifically, an oxidation peak at 1150 mV was observed to be coupled to the cathodic processes. This potential is nearly identical to that observed for the irreversible chloride oxidation of benzyltriethylammonium chloride under the same conditions. In addition, infrared spectroelectrochemical experiments reveal that **1d** is regenerated upon reduction of **5d**. Such irreversible two-electron reductions have precedent with the structurally and electronically similar $M(CO)_3(PP)X_2$ complexes referred to earlier.[27]

$$5 + 2e^- \rightarrow 1 + Cl^- \qquad (2)$$

The coupled cathodic behavior described above was characteristic of all diimine chloride complexes examined with the notable exception of **1g**, which shows only one well-defined coupled cathodic peak at a scan rate of 100 mV/s. No additional coupled peaks were observed for this complex at scan rates up to 10 000 mV/s other than that due to $\mathbf{1g}^+$. We attribute this to the generation of a single isomeric form **5g**, presumably a result of the unique steric demands of ncp.

(29) This trend is opposite to that which we observed for the rate of reaction of electrogenerated $[Mo(CO)_4(LL)]^+$ towards carbonyl substitution by acetonitrile.[26] In that system, increasing basicity of the diimine ligand had the effect of decreasing the reaction rate due stabilization of the electron-deficient molybdenum(I) toward nucleophilic attack.

(30) The electrogenerated $[Re(CO)_3(bpy)(CN)]^+$ has been reported to undergo decomposition at twice the rate of the analogous chloride;[18b] whereas we have not directly examined the cyanide complexes, their reported cyclic voltammetry responses are similar to those of the halide analogues and appear consistent with Scheme 1.

(31) Bond, A. M.; Colton, R.; McDonald, M. E. *Inorg. Chem.* **1978**, *17*, 2842–2847.

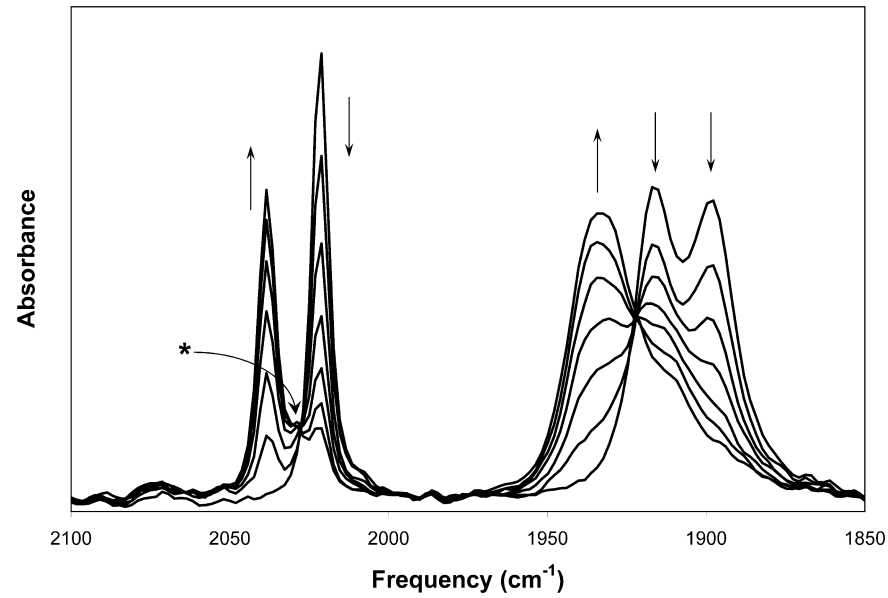

Figure 5. Infrared spectral changes in the carbonyl stretching region observed upon bulk electrolysis of **2b** in CH_3CN/TBAH. The elapsed time for the sequence is 1 min. The product is identified as **7b**; the intermediate, with peaks at 2029 (marked with the asterisk) and 1911 cm^{-1}, is assigned as $[Re(CO)_3(dmb)(\eta^1\text{-}Br_2)]^+$.

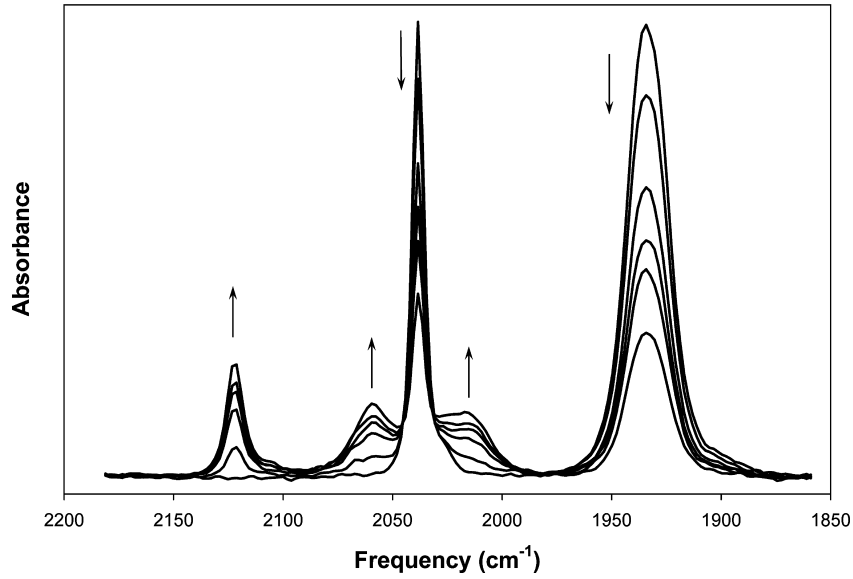

Figure 6. Infrared spectral changes in the carbonyl stretching region observed upon bulk electrolysis of **7b**(CF_3SO_3) in CH_3CN/TBAH. The elapsed time for the sequence is 3 min. The product is assigned as **7b**$^+$.

Oxidative Electrochemistry of $Re(CO)_3(LL)Br$. The cyclic voltammogram obtained for a 1.9 mM solution of **2a** at a scan rate of 100 mV/s is presented in Figure 4. The $i_{a,c}/i_{a,b}$ ratio is 0.49, consistent with the disproportionation mechanism outlined in Scheme 1. Despite this similarity, the bromide complexes show markedly different chemistry in a number of respects from the chlorides. The clearest example of this is seen in spectrolelectrochemical results obtained during the bulk oxidation of **2a** and **2b** (Figure 5). Spectral changes in the carbonyl region show nearly quantitative conversions of the starting materials to **7a** and **7b**, respectively, with yields >95% as determined by molar absorptivities. Consistent with these observations, cyclic voltammetry experiments performed at lower scan rates show substantial relative current enhancement of the coupled oxidation peaks. For example, the $i_{a,c}/i_{a,b}$ ratio for **2a** increases to 0.72 at 25 mV/s; the corresponding peak ratio for the chloride analogue, **1a**, is only 0.52 at the same scan rate.

On the basis of the above observations we propose that the electrogenerated radical cations **2**$^+$ disproportionate according to Scheme 1 but that the corresponding rhenium (III) products, **6**, subsequently decompose to yield **7** and free dibromine. Spectroelectrochemical data provide evidence that this reaction proceeds via a facial rhenium (I) tricarbonyl intermediate. Subtraction of absorbances due to **2b** and **7b** from several of the spectra shown in Figure 5 reveals peaks at 2029 (indicated with an asterisk in Figure 5) and 1911 cm^{-1}, the pattern and relative intensities of which are similar to those of **7b**, albeit with slightly lower stretching frequencies. Similarly, peaks due to an intermediate are observed at 2031 and 1914 cm^{-1} during bulk oxidation of **2a**. We assign these peaks to $[Re(CO)_3(LL)(\eta^1\text{-}Br_2)]^+$, which we

propose is generated by electron transfer from the bromide ions to the rhenium with concomitant rearrangement and formation of a dibromine bond (eq 3). Subsequent ligand substitution by the solvent then yields the corresponding acetonitrile adducts, **7a** and **7b** (eq 4). It is likely that the coupled cathodic peak (at 680 mV in Figure 4) is due to the two-electron reduction of $[Re(CO)_3(bpy)(\eta^1\text{-}Br_2)]^+$, yielding bromide and **7a** (eq 5). This assignment is supported by the observation of an anodic peak at 820 mV, attributable to free bromide, coupled to the reduction process. The markedly different stabilities of **5** and **6** are likely due to the greater polarizability of bromine compared to chlorine, which would facilitate its binding as Br_2,[32] as well as the lower oxidation potential of bromide.

$$[Re(CO)_3(LL)Br_2]^+(6) \rightarrow [Re(CO)_3(LL)(\eta^1- Br_2)]^+ \quad (3)$$

$$[Re(CO)_3(LL)(\eta^1- Br_2)]^+ + CH_3CN \rightarrow [Re(CO)_3(LL)(CH_3CN)]^+(7) + Br_2(4)$$

$$[Re(CO)_3(LL)(\eta^1- Br_2)]^+ + 2\ e^- + CH_3CN \rightarrow [Re(CO)_3(LL)(CH_3CN)]^+(7) + 2\ Br^-(5)$$

Infrared Characterization of $[Re(CO)_3(LL)(CH_3CN)]^{2+}$ Complexes. Given the marked reversibility of the oxidation of the acetonitrile adducts, **7**, a characteristic shared by many $[Re(CO)_3(LL)L']^+$ complexes when L′ is a nitrogen donor ligand,[2,15] it appeared that characterization of the seventeen-electron radical cations, $\mathbf{7}^+$, via room-temperature spectroelectrochemistry should be possible. This indeed was the case. Spectral changes observed upon oxidation of the triflate salt of **7b** are presented in Figure 6 and are representative of those obtained for all other species examined; thin-layer electrolyses typically proceeded with isosbestic conversion until approximately 50−70% of the starting compound was consumed. The substantial increase in carbonyl stretching frequencies observed upon oxidation, averaging about 90 cm^{-1}, is consistent with the generation of a rhenium (II) carbonyl.[33] In addition, the degenerate E stretching mode of the rhenium (I) starting material appears to split into distinct bands in the radical cation, perhaps due to a decrease in symmetry. We observed a similar splitting of the E band upon oxidation of the isostructural $Mo(CO)_3(LL)(CH_3CN)$,[26] and there have been other reports of significant broadening or peak splitting in related systems.[17,34] Infrared data are summarized in Table 3 and, to our knowledge, represent the first reported infrared data on radical cations derived from luminescent rhenium tricarbonyl complexes.

Conclusions

We have demonstrated that the one-electron oxidation products of luminescent $Re(CO)_3(\alpha\text{-diimine})X$ complexes **1** and **2** undergo rapid disproportionation in acetonitrile, the rates for which are influenced by the basicity and steric properties of the diimine ligand. This is a new interpretation of the frequently reported cyclic voltammetric responses of these compounds. An inner-sphere mechanism is proposed, as disproportionation is accompanied by a halide-transfer and ultimately yields **7** and rhenium (III) tricarbonyl complexes **5** or **6**. The chlorides, **5**, are stable on the thin-cell bulk electrolysis time scale and have been spectroscopically characterized. The bromides, **6**, react rapidly in acetonitrile and yield **7** and Br_2. The disproportionation of $\mathbf{1}^+$ and $\mathbf{2}^+$ are examples of a more general susceptibility of electrogenerated rhenium (II) tricarbonyl complexes to nucleophilic attack, additional work concerning which is ongoing in our laboratory.

Acknowledgment. This work was supported in part by Vermont EPSCoR, administered by the National Science Foundation, and a grant from the M. J. Murdock Charitable Trust (to the CWU Department of Chemistry). Funds to purchase the electrochemical workstation and FTIR spectrometer were made available by a generous gift to Bennington College by Kate Merck (Bennington College, '46) and Al Merck.

IC800530N

(32) Vasilyev, A. V.; Lindeman, S. V.; Kochi, J. K. *New J. Chem.* **2002**, *26*, 582–592.

(33) Baird, M. C. *Chem. Rev.* **1988**, *88*, 1217–1227.

(34) Farrell, I. R.; Hartl, F.; Záliš, S.; Wanner, M.; Kaim, W.; Vlček, A., Jr. *Inorg. Chim. Acta* **2001**, *318*, 143–151.